CHAPTER

3 BINARY MACHINE VISION

Region Analysis

3.1 Introduction

The analysis phase of binary machine vision consists of computing global properties for each region produced by the connected components labeling algorithm or each segment produced by the signature segmentation. The properties of each region or segment are stored as a measurement vector that is the input to a classifier. This chapter describes the computation of properties from regions and segments. The next chapter provides an introduction to the classification of these property vectors by statistical pattern recognition. Structural matching, another classification technique, is described in Chapter 17.

3.2 Region Properties

The connected components labeling operator produces regions. A variety of property measurements can be made on each region on the basis of the region's shape and the gray level values for those pixels that participate in the region. The gray level values for all pixels in a region give rise to a histogram of the gray level values of the region, just as all the pixels in an image give rise to the histogram of the image. Mean gray level value is only one summary statistic of the histogram. Variance, skewness, and kurtosis are other statistics of the region's gray levels. Co-occurrence measures of the region's spatial distribution of gray levels constitute summary statistics about a region's microtexture.

Other properties include its gray level spatial second moments, its area, its bounding rectangle, its extremal points, its second central moments, and its orientation. The gray level spatial second moments can measure the degree to which a region is shaded, with one side slightly brighter than the other. It can also measure the orientation of the shading. The bounding rectangle of a region is the smallest

rectangle—with sides oriented parallel to the row and column axes of the image—that contains or circumscribes the region. The region has eight extremal points: leftmost bottom, leftmost top, rightmost bottom, rightmost top, topmost left, topmost right, bottommost left, and bottommost right. A region has shape properties, such as area, number of holes, length of perimeter, length of major and minor axes of best fitting ellipse, and orientation of major axis.

In the discussion that follows, we denote the set of pixels in a region by R. Simple global properties include the region's area A and centroid $(\bar{r}, \bar{c})$. Assuming square pixels, we define these properties by

Area:

$$A = \sum_{(r,c)\in R} 1$$

Centroid:

$$\bar{r} = \frac{1}{A} \sum_{(r,c)\in R} r$$

$$\bar{c} = \frac{1}{A} \sum_{(r,c)\in R} c$$

Note that even though each $(r,c) \in R$ is a pair of integers, $(\bar{r}, \bar{c})$ is generally not a pair of integers.

The length of the perimeter P of a region is another global property. A simple definition of the perimeter of a region without holes is the sequence of its interior border pixels. A pixel of a region is a border pixel if it has some neighboring pixel that is outside the region. When 8-connectivity is used to determine whether a pixel inside the region is connected to a pixel outside the region, the resulting set of perimeter pixels is 4-connected. When 4-connectivity is used to determine whether a pixel inside the region is connected to a pixel outside the region, the resulting set of perimeter pixels is 8-connected. This motivates the following definition for the 4-connected perimeter P_4 and the 8-connected perimeter P_8 of a region R.

$$P_4 = \{(r,c) \in R | N_8(r,c) - R \neq \emptyset\}$$
$$P_8 = \{(r,c) \in R | N_4(r,c) - R \neq \emptyset\}$$

To compute length $|P|$ of perimeter P, the pixels in P must be ordered in a sequence $P =< (r_o, c_o), \ldots, (r_{K-1}, c_{K-1}) >$, each pair of successive pixels in the sequence being neighbors, including the first and last pixels. Then

$$|P| = \#\{k | (r_{k+1} c_{k+1}) \in N_4(r_k, c_k)\} + \sqrt{2}\#\{k | (r_{k+1}, c_{k+1}) \in N_8(r_k, c_k) - N_4(r_k, c_k)\}$$

where $k + 1$ is computed modulo K.

The length of the perimeter $\|P\|$ squared divided by the area (A) is sometimes used as a measure of a shape's compactness or circularity. However, Rosenfeld (1974) shows that for digital shapes, $\|P\|^2/A$ assumes its smallest value not for digital circles, as it would for continuous planar shapes, but for digital octagons or diamonds, depending on whether the perimeter is computed as the number of its 4-neighboring border pixels or as the length of its border, counting 1 for vertical or

horizontal moves and $\sqrt{2}$ for diagonal moves. Other common properties computed for a shape include the radius of its circumscribing circle, the radius of its maximal inscribed circle, the mean distance μ_R from the centroid to the shape boundary, and the standard deviation σ_R of the distances from the centroid to the shape boundary. The properties μ_R and σ_R can be defined in terms of the pixels (r_k, c_k), $k = 0, \ldots, K-1$ in the perimeter P.

$$\mu_R = \frac{1}{K} \sum_{k=0}^{K-1} \|(r_k, c_k) - (\bar{r}, \bar{c})\|$$

$$\sigma_R^2 = \frac{1}{K} \sum_{k=0}^{K-1} [\|(r_k, c_k) - (\bar{r}, \bar{c})\| - \mu_R]^2$$

Haralick (1974) shows that μ_R/σ_R has the following properties:

1. As the digital shape becomes more circular, the measure μ_R/σ_R increases monotonically.
2. The values of μ_R/σ_R for similar digital and continuous shapes are similar.
3. It is orientation and area independent.

Furthermore, the number N of sides to a regular digital polygon can be estimated from the circularity measure μ_R/σ_R by the relation

$$N = 1.4111 \left(\frac{\mu_R}{\sigma_R}\right)^{.4724}$$

We can determine for each region R its gray level mean μ and its gray level variance σ^2. The gray level mean is a first-order property. The gray level variance is a second-order property. Average gray level:

$$\mu = \frac{1}{A} \sum_{(r,c) \in R} I(r,c)$$

Gray level variance:

$$\sigma^2 = \frac{1}{A} \sum_{(r,c) \in R} [I(r,c) - \mu]^2 = \left[\frac{1}{A} \sum_{(r,c) \in R} I(r,c)^2\right] - \mu^2$$

We can determine for each region R some microtexture properties that are a function of the region's co-occurrence matrix. Let S be a set of all pairs of pixels in the region R that are in a designated spatial relationship. For example, S could be the set of all pairs of pixels in R that are 4-neighbors. Define the region's co-occurrence matrix P by

$$P(g_1, g_2) = \frac{\#\{[(r_1, c_1), (r_2, c_2)] \in S \mid I(r_1, c_1) = g_1 \text{and } I(r_2, c_2) = g_2\}}{\#S}$$

Common texture features include the texture second moment M, the entropy E, the

correlation ρ, the contrast C, and the homogeneity H (Haralick, Shanmugam, and Dinstein, 1973). They can all be defined in terms of the co-occurrence P:

$$M = \sum_{g_1, g_2} P^2(g_1, g_2)$$

$$E = -\sum_{g_1, g_2} P(g_1, g_2) \log P(g_1, g_2)$$

$$\rho = \sum_{g_1, g_2} (g_1 - \mu)(g_2 - \mu) P(g_1, g_2)/\sigma^2$$

where

$$\mu = \frac{1}{2}\left[\sum_{g_1}\sum_{g_2} g_1 P(g_1, g_2) + \sum_{g_1}\sum_{g_2} g_2 P(g_1, g_2)\right]$$

$$\sigma^2 = \frac{1}{2}\left[\sum_{g_1}\sum_{g_2} (g_1 - \mu)^2 P(g_1, g_2) + \sum_{g_1}\sum_{g_2} (g_2 - \mu)^2 P(g_1, g_2)\right]$$

$$C = \sum_{g_1}\sum_{g_2} |g_1 - g_2| P(g_1, g_2)$$

$$H = \sum_{g_1}\sum_{g_2} \frac{P(g_1, g_2)}{k + |g_1 - g_2|} \qquad \text{where } k \text{ is some small constant}$$

Other features can be found in Gleason and Agin (1979) and Pavlidis (1977).

For each region, we can determine properties that relate to its shape and orientation. The first-order measurements that relate to shape and orientation can be derived from the region's extremal pixels. Second-order measurements that relate to shape and orientation can be obtained from the second order spatial moments. First we will discuss a region's extremal pixels and some shape properties computable from them. Then we will discuss a region's second order spatial moments and the properties computable from them.

3.2.1 Extremal Points

As shown in Fig. 3.1, there can be as many as eight distinct extremal pixels to a region: topmost right, rightmost top, rightmost bottom, bottommost right, bottommost left, leftmost bottom, leftmost top, and topmost left. Each extremal point has an extremal coordinate value in either its row or column coordinate position. Each extremal point lies on the normally oriented bounding rectangle of the region. This too is shown in Fig. 3.1. Figure 3.2 shows two simple regions in which different extremal points may be coincident. For example, in the rectangle the topmost right extremal point and the rightmost top extremal point are coincident. In the elongated diamond the topmost right and the topmost left extremal points are coincident.

To help discuss and mathematically define the extremal points of a region, we use the associations given in Table 3.1.

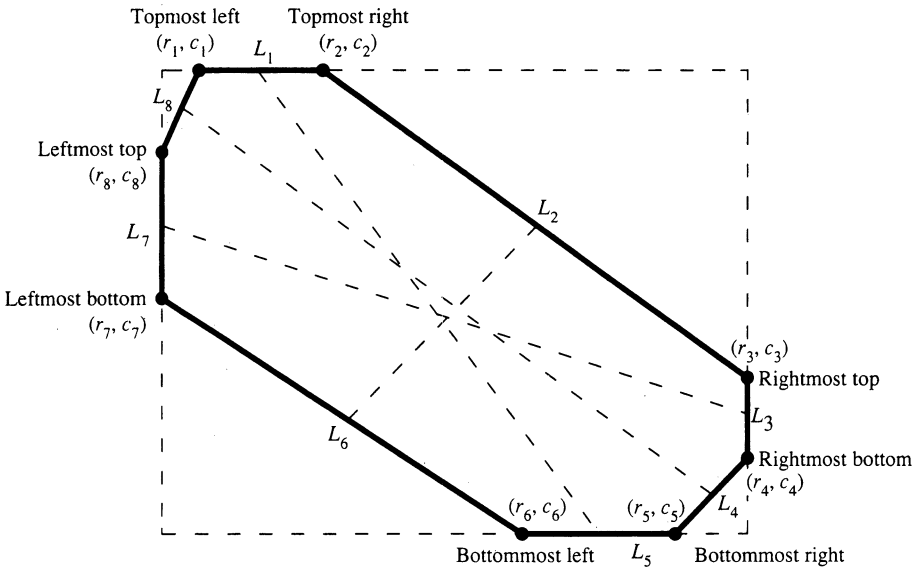

Figure 3.1 The eight extremal points a region can have and the normally oriented bounding rectangle that encloses the region. The interior dotted lines pair together opposite sides.

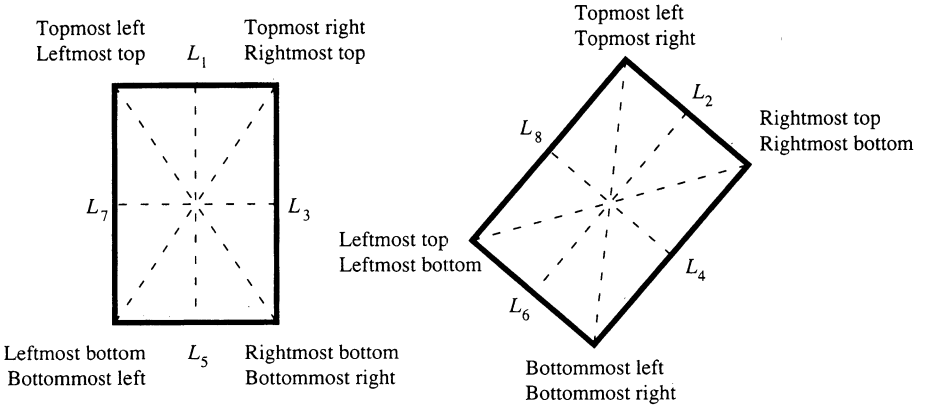

Figure 3.2 Two regions in which the extremal points are not unique and in which they pair differently. The interior dotted lines pair together opposite sides. Because some extremal points are coincident, some opposite sides have zero length.

Table 3.1 Association of the name of the eight extremal points with their coordinate representation.

Name of Extremal Point	Coordinate Representation
Topmost left	(r_1, c_1)
Topmost right	(r_2, c_2)
Rightmost top	(r_3, c_3)
Rightmost bottom	(r_4, c_4)
Bottommost right	(r_5, c_5)
Bottommost left	(r_6, c_6)
Leftmost bottom	(r_7, c_7)
Leftmost top	(r_8, c_8)

Let R be the given region. The extremal points of R can be defined in terms of the topmost row, *rmin,* of R; the bottommost row, *rmax,* of R; the leftmost column, *cmin,* of R; and the rightmost column, *cmax,* of R. The definitions for these extremal coordinates are given in Table 3.2.

Now we can directly define the coordinates of the extremal points:

$$r_1 = r_2 = rmin \qquad r_5 = r_6 = rmax$$
$$c_1 = \min\{c|(\text{rmin}, c) \in R\} \qquad c_5 = \max\{c|(\text{rmax}, c) \in R\}$$
$$c_2 = \max\{c|(\text{rmin}, c) \in R\} \qquad c_6 = \min\{c|(\text{rmax}, c) \in R\}$$
$$r_3 = \min\{r|(r, \text{cmax}) \in R\} \qquad r_7 = \max\{r|(r, \text{cmin}) \in R\}$$
$$r_4 = \max\{r|(r, \text{cmax}) \in R\} \qquad r_8 = \min\{r|(r, \text{cmin}) \in R\}$$
$$c_3 = c_4 = cmax \qquad c_7 = c_8 = cmin$$

Table 3.2 Association of the name of an extremal coordinate with its definition.

Name of Extremal Coordinate	Coordinate Representation and Definition
Topmost row	$\text{rmin} = \min\{r|(r, c) \in R\}$
Bottommost row	$\text{rmax} = \max\{r|(r, c) \in R\}$
Leftmost column	$\text{cmin} = \min\{c|(r, c) \in R\}$
Rightmost column	$\text{cmax} = \max\{c|(r, c) \in R\}$

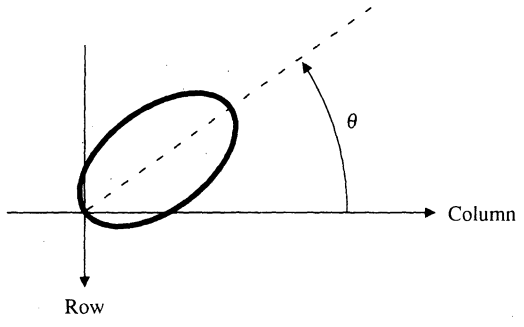

Figure 3.3 The eight extremal points a region can have and the normally oriented bounding rectangle that encloses the region. The interior dotted lines pair together opposite extremal points. They constitute the axes M_1, M_2, M_3, and M_4.

Extremal points occur in opposite pairs: topmost left with bottommost right; topmost right with bottommost left; rightmost top with leftmost bottom; and rightmost bottom with leftmost top. Each pair of opposite extremal points defines an axis. Useful properties of the axis include its axis length and orientation. Because the extremal points come from a spatial digitization or quantization, the standard Euclidean distance formula will provide distances that are biased slightly low. (Consider, for example, the length covered by two pixels horizontally adjacent. From the left edge of the left pixel to the right edge of the right pixel is a length of 2, but the distance between the pixel centers is only 1.) The appropriate calculation for distance adds a small increment to the Euclidean distance to account for this. The increment depends on the orientation angle of the axis. Letting these respective axes be M_1, M_2, M_3, and M_4, where M_1 is the axis between extremal points (r_1, c_1) and (r_5, c_5), M_2 is the axis between extremal points (r_2, c_2) and (r_6, c_6), M_3 is the axis between extremal points (r_3, c_3) and (r_7, c_7), and M_8 is the axis between extremal points (r_4, c_4) and (r_8, c_8) (Fig. 3.3), we have

$$\begin{aligned} M_1 &= \sqrt{(r_1 - r_5)^2 + (c_1 - c_5)^2} + Q(\phi_1) \\ M_2 &= \sqrt{(r_2 - r_6)^2 + (c_2 - c_6)^2} + Q(\phi_2) \\ M_3 &= \sqrt{(r_3 - r_7)^2 + (c_3 - c_7)^2} + Q(\phi_3) \\ M_4 &= \sqrt{(r_4 - r_8)^2 + (c_4 - c_8)^2} + Q(\phi_4) \end{aligned} \tag{3.1}$$

The axes M_1, M_2, M_3, and M_4 have orientations ϕ_1, ϕ_2, ϕ_3, and ϕ_4, where the orientation of a line segment taken counterclockwise with respect to the column (horizontal) axis as shown in Fig. 3.4 is defined by

$$\phi_1 = \tan^{-1} \frac{r_1 - r_5}{-(c_1 - c_5)}$$

$$\phi_2 = \tan^{-1} \frac{r_2 - r_6}{-(c_2 - c_6)}$$

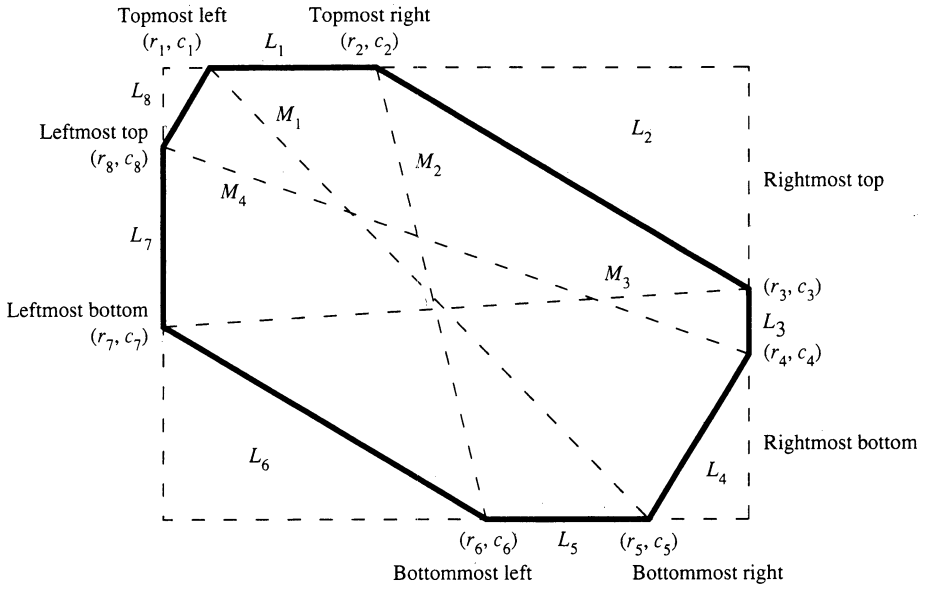

Figure 3.4 Orientation convention for the axes. The orientation angle of an axis is measured counterclockwise from the column axis.

$$\phi_3 = \tan^{-1} \frac{r_3 - r_7}{-(c_3 - c_7)} \tag{3.2}$$

$$\phi_4 = \tan^{-1} \frac{r_4 - r_8}{-(c_4 - c_8)}$$

The exact value for $Q(\theta)$ as shown in Fig. 3.5 is given by

$$Q(\theta) = \begin{cases} \frac{1}{|\cos\theta|} & \text{if } |\theta| < 45° \\ \frac{1}{|\sin\theta|} & \text{if } |\theta| > 45° \end{cases} \tag{3.3}$$

If a quick calculation for distance needs to be done, the average value 1.12 can be used for $Q(\theta)$. The largest error incurred for this approximation is .294.

The axes are also paired: M_1 with its mate M_3, and M_2 with its mate M_4. Major and minor axes of thin elongated or linelike regions can be determined from M_1, M_2, M_3, and M_4. The major axis will be the one having length $\max\{M_1, M_2, M_3, M_4\}$. The minor axis will be its mate. When the major axis is not unique, the minor axis will be the shortest among the axes mating to the longest-length axis. An example is shown in Fig. 3.6. There the major axis is $M_1 = M_2 = M_3$. The minor axis is M_4, and it will, in general, be longer than the width of the region since it is not necessarily orthogonal to the major axis. The width of the region can, however, be estimated by multiplying the minor axis by the absolute value of the size of the difference in the orientation of the major and minor axes.

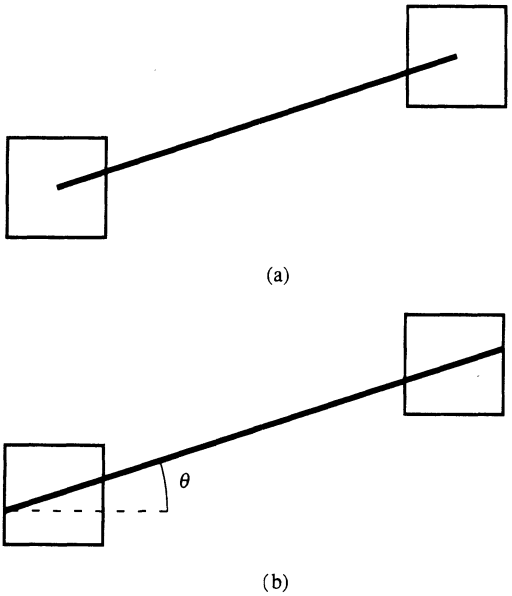

Figure 3.5 Diagram showing why the distance between two pixels must be increased if it is to count length going from the left edge of the left pixel to the right edge of the right pixel. Part (a) shows the distance between pixel centers; (b) shows the left edge to right edge distance. Each pixel must add a length that is the length of the hypotenuse of a right triangle having base 1/2. For $|\theta| < 45°$, this length is $1/2 \cos\theta$ for each pixel.

To characterize elongated triangular shapes, the distances between all pairs of extremal points must be computed. The extremal point having the greatest sum of its two largest distances to other extremal points can be selected as the apex of the triangle. The two other extremal points then constitute the vertices at the base of the triangle. To be more precise, define the distance between the ith and jth extremal point by

$$M_{ij} = \sqrt{(r_i - r_j)^2 + (c_i - c_j)^2} + 1.12$$

Let k_1, k_2, and k_3 be any indices maximizing $M_{k_1k_2} + M_{k_1k_3}$. Then the vertices of the triangle are (r_{k_1}, c_{k_1}), (r_{k_2}, c_{k_2}), and (r_{k_3}, c_{k_3}).

For a triangle known to be an isosceles triangle, the length L of the long sides can be estimated by $L = (M_{k_1k_2} + M_{k_1k_2})/2$, and the length B of the base can be estimated by $B = M_{k_2k_3}$. From the geometry of the isosceles triangle, the height of altitude h is given by

$$h = \sqrt{L^2 - \left(\frac{B}{2}\right)^2}$$

The orientation of the isosceles triangle can be estimated as the orientation ϕ_h of its

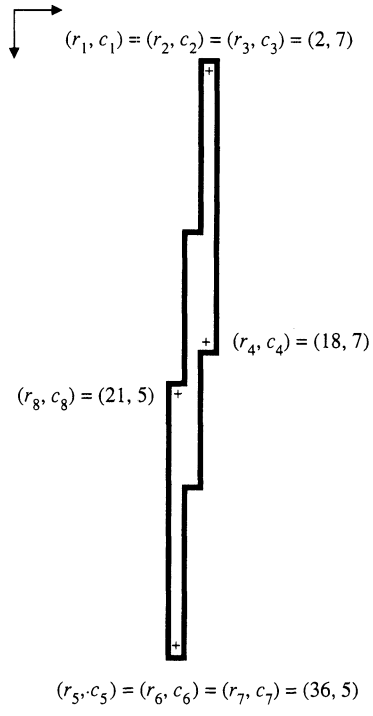

$$M_1 = M_2 = M_3 = \sqrt{(2-36)^2 + (7-5)^2)} + 1.12 = 35.18$$
$$M_4 = \sqrt{(18-21)^2 + (7-5)^2} + 1.12 = 4.73$$
$$\phi_1 = \phi_2 = \phi_3 = \tan^{-1}\frac{-34}{-(2)} = -93.37°$$

Figure 3.6 Calculation of the axis length and orientation of a linelike shape.

altitude, which is given by

$$\phi_h = \tan^{-1}\frac{\frac{1}{2}(r_{k_2} + r_{k_3}) - r_{k_1}}{-[\frac{1}{2}(c_{k_2} + c_{k_3}) - c_{k_1}]}$$

Figure 3.7 illustrates these calculations for an example isosceles triangle.

The orientation for square and rectangular shapes can also be determined from M_1, M_2, M_3, M_4 and ϕ_1, ϕ_2, ϕ_3, ϕ_4. From the geometry of Fig. 3.8 it is apparent that the two longest axes of M_1, M_2, M_3, and M_4 are the diagonals of the square or rectangle and that these two longest axes are mates. Denote the length of the longest axis by $M_{(1)}$. Let the length of its mate be $M_{m(1)}$. Denote the orientation of the longest axis by $\phi_{(1)}$. Let the orientation of its mate be $\phi_{m(1)}$. From Fig. 3.8,

$$\phi_1 = 180 + \theta_R + \alpha \quad \phi_2 = 180 + \theta_R + \alpha$$
$$\phi_3 = 180 + \theta_R - \alpha \quad \phi_4 = 180 + \theta_R - \alpha \tag{3.4}$$

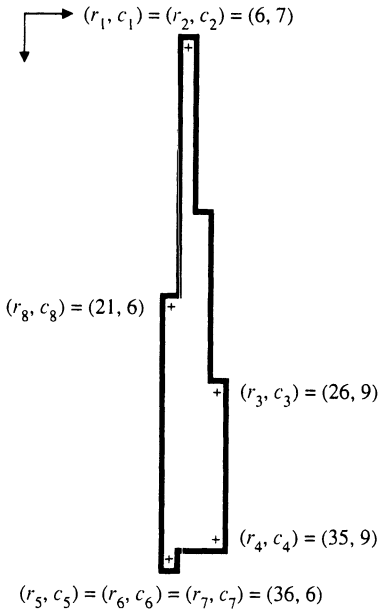

$$M_{13} = M_{23} = \sqrt{(6-26)^2 + (7-9)^2} + 1.12 = 21.22$$
$$M_{14} = M_{24} = \sqrt{(6-35)^2 + (7-9)^2} + 1.12 = 30.19$$
$$M_{15} = M_{25} = M_{16} = M_{26} = M_{17} = M_{27} = \sqrt{(6-36)^2 + (7-6)^2} + 1.12 = 31.14$$
$$M_{18} = M_{28} = \sqrt{(6-21)^2 + (7-6)^2} + 1.12 = 16.15$$
$$M_{34} = \sqrt{(26-35)^2 + (9-9)^2} + 1.12 = 10.12$$
$$M_{35} = M_{36} = M_{37} = \sqrt{(26-36)^2 + (9-6)^2} + 1.12 = 11.56$$
$$M_{38} = \sqrt{(26-21)^2 + (9-6)^2} + 1.12 = 6.95$$
$$M_{45} = M_{46} = M_{47} = \sqrt{(35-36)^2 + (9-6)^2} + 1.12 = 4.28$$
$$M_{48} = \sqrt{(35-21)^2 + (9-6)^2} + 1.12 = 15.44$$
$$M_{58} = M_{68} = M_{78} = \sqrt{(36-21)^2 + (6-6)^2} + 1.12 = 16.42$$

$$k_1 = 1, \quad k_2 = 4, \quad k_3 = 5$$
$$L = 30.67$$
$$B = 4.28$$
$$h = 30.60$$
$$\phi_h = \tan^{-1} \frac{\frac{1}{2}(35+36)-6}{-(\frac{1}{2}(9+6)-7)}$$
$$= \tan^{-1} \frac{29.5}{-.5}$$
$$= 90.97°$$

Figure 3.7 Calculations for length of sides, base, and altitude for an example isosceles triangle.

Hence, regardless who the mates are, the orientation θ_R of the rectangle is given by

$$\theta_R = \frac{\phi_1 + \phi_{m1}}{2} - 180 \tag{3.5}$$

where θ_R is the counterclockwise angle to the first side encountered from the horizontal axis and $0° \leq \theta_R \leq 90°$.

Care must be used in the computation of ϕ_1 and ϕ_3, which are defined by Eq. (3.4). The topmost, bottommost, leftmost, and rightmost vertices must be associated with coordinates exactly as shown in Fig. 3.8 and used in Eq. (3.1). The

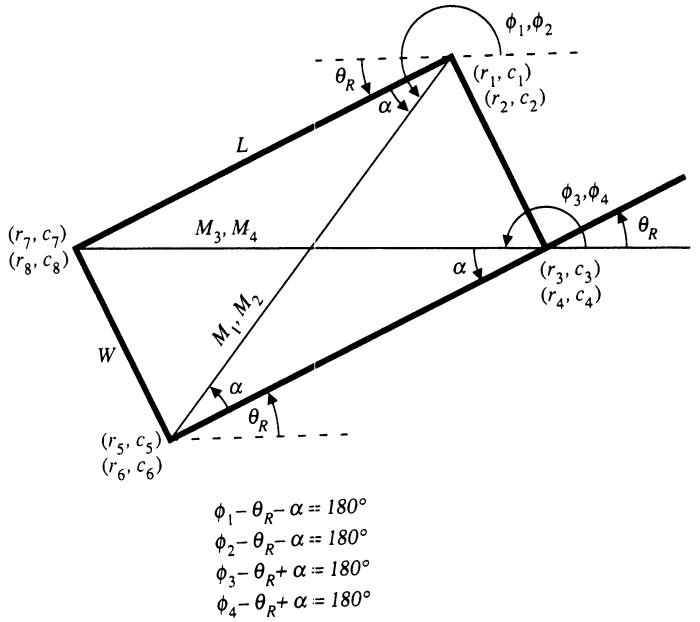

Figure 3.8 Geometry of the tilted rectangle. The diagram shows the relationship between the angular orientation θ_R and the angles of the axes joining opposite pairs of extremal points. Here (r_1, c_1) is the topmost vertex; (r_3, c_3) the rightmost vertex; (r_5, c_5) the bottommost vertex; and (r_7, c_7) the leftmost vertex.

relationship given in Eq. (3.5) is the relation when $\phi_1 > 0$ and $\phi_3 > 0$. Should ϕ_1 or ϕ_3 be computed as a negative value from the arctangent function, 360° must be added to it to make it positive before it can be used in Eq. (3.5). Shown in Fig. 3.9 is an example calculation.

Also from Eq. (3.4), the included angle α between the rectangle side and the diagonal is given by

$$\alpha = \min\left\{\frac{|\phi_{(1)} - \phi_{m(1)}|}{2}, 180 - \frac{|\phi_1 - \phi_{m1}|}{2}\right\}$$

The length L and width W of the rectangle are functions of α :

$$L = \frac{M_{(1)} + M_{m(1)}}{2} \cos\alpha$$

$$W = \frac{M_{(1)} + M_{m(1)}}{2} \sin\alpha$$

We can define the line segment lengths $L_1, \ldots, L_8$ between successive pairs of extremal points as shown in Fig. 3.10. These lengths can form the basis of the description of octagonal shapes in terms of their axes. There are four possible axes for octagonal-shaped regions. Each axis has a length and an orientation. The dominant axis will be taken to be the major axis of the region, and its orientation

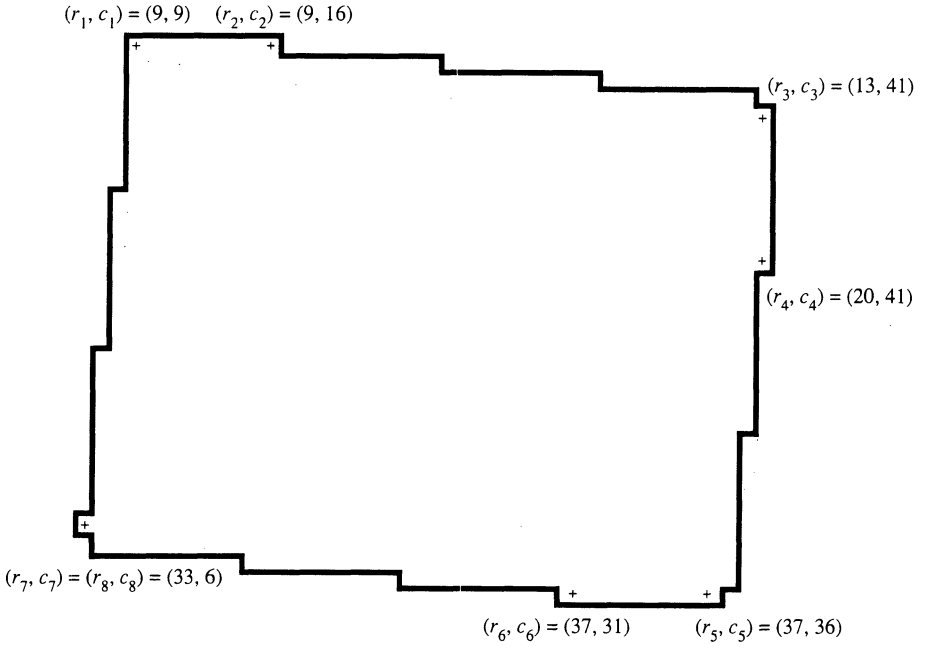

$$M_1 = \sqrt{(9-37)^2 + (9-38)^2} + 1.12 = 41.43$$
$$M_2 = \sqrt{(9-37)^2 + (16-31)^2} + 1.12 = 32.88$$
$$M_3 = \sqrt{(13-33)^2 + (41-6)^2} + 1.12 = 41.43$$
$$M_4 = \sqrt{(20-33)^2 + (41-6)^2} + 1.12 = 38.46$$

$$M_{(1)} = M_1$$

$$M_{m(1)} - M_3$$

$$\phi_{(1)} = \tan^{-1}\frac{r_1 - r_5}{-(c_1 - c_5)} = \tan^{-1}\frac{9-37}{-(9-38)} \quad \tan^{-1}\frac{-28}{29} = -43.99°$$

$$\phi_{m(1)} = \tan^{-1}\frac{r_3 - r_7}{-(c_3 - c_7)} = \tan^{-1}\frac{13-33}{-(41-6)} \quad \tan^{-1}\frac{-20}{-35} = -150.26°$$

$$\theta_R = \frac{\phi_{(1)} + \phi_{m(1)}}{2} + 90° = -7.13°$$

Figure 3.9 Calculation for the orientation of an example rectangle.

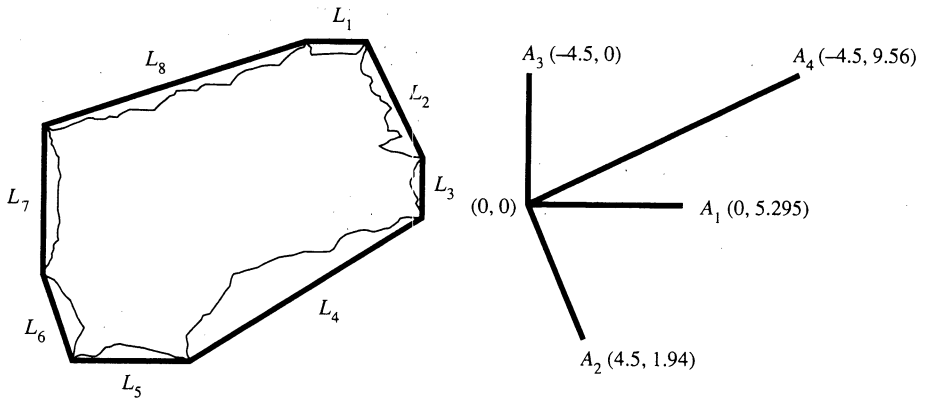

Side length	Extremal point	Axis length	Axis orientation
$L_1 = 3$	$(r_1, c_1) = (2, 13)$	A_1:5.295	0°
$L_2 = 5.51$	$(r_2, c_2) = (2, 15)$	A_2:4.935	−66.9°
$L_3 = 3$	$(r_3, c_3) = (6, 17)$	A_3:4.5	90°
$L_4 = 10.55$	$(r_4, c_4) = (8, 17)$	A_4:10.575	25.2°
$L_5 = 5$	$(r_5, c_5) = (13, 9)$		
$L_6 = 4.28$	$(r_6, c_6) = (13, 5)$		
$L_7 = 6$	$(r_7, c_7) = (10, 4)$		
$L_8 = 10.6$	$(r_8, c_8) = (5, 4)$		

Figure 3.10 Axes and their mates that arise from octagonal-shaped regions and their extremal points.

will be the orientation of the region. The line segment lengths are defined by:

$$L_1 = |c_1 - c_2| + 1$$
$$L_2 = \sqrt{(r_2 - r_3)^2 + (c_2 - c_3)^2} + Q(\theta_2)$$
$$L_3 = |r_3 - r_4| + 1$$
$$L_4 = \sqrt{(r_4 - r_5)^2 + (c_4 - c_5)^2} + Q(\theta_4)$$
$$L_5 = |c_5 - c_6| + 1$$
$$L_6 = \sqrt{(r_6 - r_7)^2 + (c_6 - c_7)^2} + Q(\theta_2)$$
$$L_7 = |r_7 - r_8| + 1$$
$$L_8 = \sqrt{(r_8 - r_1)^2 + (c_8 - c_1)^2} + Q(\theta_4)$$

The lengths of the four axes are denoted by A_1, A_2, A_3, and A_4. They are

determined by

$$A_1 = \frac{(L_1 + L_5)}{2}$$

$$A_2 = \frac{(L_2 + L_6)}{2}$$

$$A_3 = \frac{(L_3 + L_7)}{2}$$

$$A_4 = \frac{(L_4 + L_8)}{2}$$

Axes for each region occur in mating pairs: A_1 with A_3, and A_2 with A_4. The major axis is the one having the largest length. The minor axis is its axis mate. These axes are different from M_1, M_2, M_3, and M_4.

The orientation angle for A_1 is always 0°, since the line segments that define it are horizontal, and the orientation angle for A_3 is always 90°, since the line segments that define it are always vertical. The counterclockwise orientation angle for A_2 is given by

$$\theta_2 = \frac{1}{2A_2}\left[L_2 \tan^{-1}\frac{r_2 - r_3}{-(c_2 - c_3)} + L_6 \tan^{-1}\frac{r_7 - r_6}{-(c_7 - c_6)}\right]$$

The orientation angle for A_4 is given by

$$\theta_4 = \frac{1}{2A_4}\left[L_4 \tan^{-1}\frac{r_4 - r_5}{-(c_4 - c_5)} + L_8 \tan^{-1}\frac{r_1 - r_8}{-(c_1 - c_8)}\right]$$

3.2.2 Spatial Moments

There are three second-order spatial moments of a region. They are denoted by μ_{rr}, μ_{rc}, and μ_{cc} and are defined as follows:

Second-order row moment: $$\mu_{rr} = \frac{1}{A}\sum_{(r,c)\in R}(r - \bar{r})^2$$

Second-order mixed moment: $$\mu_{rc} = \frac{1}{A}\sum_{(r,c)\in R}(r - \bar{r})(c - \bar{c})$$

Second-order column moment: $$\mu_{cc} = \frac{1}{A}\sum_{(r,c)\in R}(c - \bar{c})^2$$

The second spatial moments have value and meaning for a region of any shape, the same way that the covariance matrix has value and meaning for any two-dimensional probability distribution. If the region is an ellipse, an algebraic meaning can be given to the second spatial moments.

If a region R is an ellipse whose center is the origin, then R can be expressed as

$$R = \{(r, c) \mid dr^2 + 2erc + fc^2 \leq 1\}$$

A relationship exists between the coefficients d, e, and f of the equation of the ellipse and the second moments μ_{rr}, μ_{rc}, and μ_{cc}, as shown in Appendix A. It is given by

$$\begin{pmatrix} d & e \\ e & f \end{pmatrix} = \frac{1}{4(\mu_{rr}\mu_{cc} - \mu_{rc}^2)} \begin{pmatrix} \mu_{cc} & -\mu_{rc} \\ -\mu_{rc} & \mu_{rr} \end{pmatrix}$$

Since the coefficients d, e, and f determine the lengths of the major and minor axes and the orientation of the ellipse, this relationship means that the second moments μ_{rr}, μ_{rc}, and μ_{cc} also determine the lengths of the major and minor axes and the orientation of the ellipse.

To determine the lengths of the major and minor axes and their orientations from the second-order moments, we must consider four cases. These are discussed in Appendix A and are summarized here:

1. $\mu_{rc} = 0$ and $\mu_{rr} > \mu_{cc}$

The major axis is oriented at an angle of $-90°$ counterclockwise from the column axis and has a length of $4\mu_{rr}^{1/2}$. The minor axis is oriented at an angle of $0°$ counterclockwise from the column axis and has a length of $4\mu_{cc}^{1/2}$.

2. $\mu_{rc} = 0$ and $\mu_{rr} \leq \mu_{cc}$

The major axis is oriented at an angle of $0°$ counterclockwise from the column axis and has a length of $4\mu_{cc}^{1/2}$. The minor axis is oriented at an angle of $-90°$ counterclockwise from the column axis and has a length of $4\mu_{rr}^{1/2}$.

3. $\mu_{rc} \neq 0$ and $\mu_{rr} \leq \mu_{cc}$

The major axis is oriented at an angle of

$$\tan^{-1}\left\{\frac{-2\mu_{rc}}{\mu_{rr} - \mu_{cc} + \left[(\mu_{rr} - \mu_{cc})^2 + 4\mu_{rc}^2\right]^{1/2}}\right\}$$

counterclockwise with respect to the column axis and has a length of

$$\left[8\left\{\mu_{rr} + \mu_{cc} + \left[(\mu_{rr} - \mu_{cc})^2 + 4\mu_{rc}^2\right]^{1/2}\right\}\right]^{1/2}$$

The minor axis is oriented at an angle $90°$ counterclockwise from the major axis and has a length of

$$\left[8\left\{\mu_{rr} + \mu_{cc} - \left[(\mu_{rr} - \mu_{cc})^2 + 4\mu_{rc}^2\right]^{1/2}\right\}\right]^{1/2}$$

4. $\mu_{rc} \neq 0$ and $\mu_{rr} > \mu_{cc}$

The major axis is oriented at an angle of

$$\tan^{-1}\frac{\left[\left\{\mu_{cc} + \mu_{rr} + \left[(\mu_{cc} - \mu_{rr})^2 + 4\mu_{rc}^2\right]^{1/2}\right\}\right]^{1/2}}{-2\mu_{rc}}$$

counterclockwise with respect to the column axis and has a length of

$$\left[8\left\{\mu_{rr}+\mu_{cc}+\left[(\mu_{rr}-\mu_{cc})^2+4\mu_{rc}^2\right]^{1/2}\right\}\right]^{1/2}$$

The minor axis is oriented at an angle of 90° counterclockwise from the major axis and has a length of

$$\left[8\left\{\mu_{rr}+\mu_{cc}-\left[(\mu_{rr}-\mu_{cc})^2+4\mu_{rc}^2\right]^{1/2}\right\}\right]^{1/2}$$

3.2.3 Mixed Spatial Gray Level Moments

Region properties include properties about the region's position, extent, and shape as well as properties about the gray levels of pixels that participate in the region. Simple gray level properties include gray level mean and variance. Other gray level properties include the mixed spatial gray level moments we discuss here.

There are two second-order mixed gray level spatial moments. They are defined by

$$\mu_{rg}=\frac{1}{A}\sum_{(r,c)\in R}(r-\bar{r})[I(r,c)-\mu]$$

$$\mu_{cg}=\frac{1}{A}\sum_{(r,c)\in R}(c-\bar{c})[I(r,c)-\mu]$$

The mixed gray level spatial moments can be used to determine the least-squares, best-fit gray level intensity planes to the observed gray level spatial pattern of the region R. The least-squares fit to the observed $I(r,c)$ is the gray level intensity plane $\alpha(r-\bar{r})+\beta(c-\bar{c})+\gamma$ determined from the α,β, and γ that minimizes

$$\epsilon^2=\sum_{(r,c)\in R}\left[\alpha(r-\bar{r})+\beta(c-\bar{c})+\gamma-I(r,c)\right]^2$$

Taking partial derivatives of ϵ^2 with respect to α,β, and γ and setting these partial derivatives to zero leads to the normal regression equation that in this instance is

$$\begin{pmatrix}\sum_{(r,c)\in R}(r-\bar{r})^2 & \sum_{(r,c)\in R}(r-\bar{r})(c-\bar{c}) & \sum_{(r,c)\in R}(r-\bar{r})\\ \sum_{(r,c)\in R}(r-\bar{r})(c-\bar{c}) & \sum_{(r,c)\in R}(c-\bar{c})^2 & \sum_{(r,c)\in R}(c-\bar{c})\\ \sum_{(r,c)\in R}(r-\bar{r}) & \sum_{(r,c)\in R}(c-\bar{c}) & \sum_{(r,c)\in R}1\end{pmatrix}\begin{pmatrix}\alpha\\ \beta\\ \gamma\end{pmatrix}=$$

$$\begin{pmatrix}\sum_{(r,c)\in R}(r-\bar{r})I(r,c)\\ \sum_{(r,c)\in R}(c-\bar{c})I(r,c)\\ \sum_{(r,c)\in R}I(r,c)\end{pmatrix}$$

Since $\sum_{(r,c)\in R}(r-\bar{r})=0$ and $\sum_{(r,c)\in R}(c-\bar{c})=0$, this system of three equations simplifies to

$$\begin{pmatrix} \sum_{(r,c)\in R}(r-\bar{r})^2 & \sum_{(r,c)\in R}(r-\bar{r})(c-\bar{c}) & 0 \\ \sum_{(r,c)\in R}(r-\bar{r})(c-\bar{c}) & \sum_{(r,c)\in R}(c-\bar{c})^2 & 0 \\ 0 & 0 & \sum_{(r,c)\in R}1 \end{pmatrix} \begin{pmatrix} \alpha \\ \beta \\ \gamma \end{pmatrix} = \begin{pmatrix} \sum_{(r,c)\in R}(r-\bar{r})(I(r,c)-\gamma) \\ \sum_{(r,c)\in R}(c-\bar{c})(I(r,c)-\gamma) \\ \sum_{(r,c)\in R}I(r,c) \end{pmatrix}$$

Hence

$$\gamma = \frac{1}{A}\sum_{(r,c)\in R} I(r,c) = \mu$$

Recalling that

$$\mu_{rr} = \frac{1}{A}\sum_{(r,c)\in R}(r-\bar{r})^2$$

$$\mu_{rc} = \frac{1}{A}\sum_{(r,c)\in R}(r-\bar{r})(c-\bar{c})$$

$$\mu_{cc} = \frac{1}{A}\sum_{(r,c)\in R}(c-\bar{c})^2$$

we know that the unknown parameters α and β must satisfy

$$\begin{pmatrix} \mu_{rr} & \mu_{rc} \\ \mu_{rc} & \mu_{cc} \end{pmatrix} \begin{pmatrix} \alpha \\ \beta \end{pmatrix} = \begin{pmatrix} \mu_{rg} \\ \mu_{cg} \end{pmatrix}$$

Now by Kramer's rule we can solve for α and β, obtaining

$$\alpha = \frac{\begin{vmatrix} \mu_{rg} & \mu_{rc} \\ \mu_{cg} & \mu_{cc} \end{vmatrix}}{\begin{vmatrix} \mu_{rr} & \mu_{rc} \\ \mu_{rc} & \mu_{cc} \end{vmatrix}}$$

and

$$\beta = \frac{\begin{vmatrix} \mu_{rr} & \mu_{rg} \\ \mu_{rc} & \mu_{cg} \end{vmatrix}}{\begin{vmatrix} \mu_{rr} & \mu_{rc} \\ \mu_{rc} & \mu_{cc} \end{vmatrix}}$$

Therefore the equation of the fitted plane is given by

$$\hat{I}(r,\ c) = \alpha(r-\bar{r}) + \beta(c-\bar{c}) + \mu, \qquad (r,\ c) \in R$$

EXAMPLE 3.1

To illustrate what connected components analysis does, consider the gray scale image shown in Fig. 2.1. It contains a background of 0. There are two line objects and three blob objects. The purpose of the image processing task is to determine the position, size, and orientation of each

- bright line,
- dark line,
- bright blob,
- dark blob.

We use the convention that dark means a low-valued gray level (less than 6 in our example) and bright means a high-valued gray level (6 or greater in our example). Notice that the processing must analyze units that are not pixels. The units of analysis are lines and blobs. The properties of these units are location, shape, and gray level. The properties of these higher level units are not the corresponding properties of pixels. However, the gray level properties of an object's pixels will determine the gray level properties of the objects to which they belong. The spatial arrangement of an object's pixels will determine the shape of the higher level unit to which they belong. The positions of the pixels will determine the positions of the higher-level unit to which they belong.

The connected components grouping operation on a binary image is a unit transformation operation. It changes the unit of analysis. The binary image for our example is shown in Fig. 2.2. All pixels greater than 0 on the original gray scale image are marked binary-1 on the thresholded image. The unit on the thresholded image is the pixel. The unit on the labeled image is the region. The regions are the maximal-sized connected groups of pixels all having the value binary 1 on the thresholded image. The connected components labeling operation assigns to each binary-1 pixel the unique label of the connected component to which it belongs. Operations that follow the connected components labeling treat the region as a unit, measuring a variety of gray level and shape properties for each region.

The connected components labeled image in Fig. 3.11 has five regions, whose names or labels are 1 through 5. Each of the five regions can be measured on the basis of several properties. Most of the properties discussed in Section 3.3 for the example are tabulated in Table 3.3. For the example problem, we use the criterion that a mean gray level less than 6 signifies a dark region and a mean gray level greater than or equal to 6 signifies a bright region. Also, we use the criterion that a major-to-minor axis ratio greater than 3 signifies a line object and a ratio less than or equal to 3 signifies a blob object. By these analysis criteria, we find that region 1 is a bright blob, region 2 is a dark line, region 3 is a bright line, region 4 is a dark blob, and region 5 is also a dark blob.

⌜								1	1	1			
									1	1	1		
		2								1	1	1	
		2									1	1	1
		2				3							
	2					3							
	2						3						
2							3						
								3					
	4	4							5	5	5	5	
	4	4							5	5	5	5	
	4	4							5	5	5	5	

Figure 3.11 Connected components labeling of the image in Fig. 2.2.

Table 3.3 All the properties measured from each of the regions determined by the connected components labeling.

Property	1	2	3	4	5
Topmost left (r_1, c_1)	(1,9)	(3,3)	(5,7)	(11,2)	(11,10)
Topmost right (r_2, c_2)	(1,11)	(3,3)	(5,7)	(11,3)	(11,13)
Rightmost top (r_3, c_3)	(4,14)	(3,3)	(9,9)	(11,3)	(11,13)
Rightmost bottom (r_4, c_4)	(4,14)	(5,3)	(9,9)	(13,3)	(13,13)
Bottommost right (r_5, c_5)	(4,14)	(8,1)	(9,9)	(13,3)	(13,13)
Bottommost left (r_6, c_6)	(4,12)	(8,1)	(9,9)	(13,2)	(13,10)

Table 3.3 *Continued.*

Property	1	2	3	4	5
Leftmost bottom (r_7, c_7)	(1,9)	(8,1)	(6,7)	(13,2)	(13,10)
Leftmost top (r_8, c_8)	(1,9)	(8,1)	(5,7)	(11,2)	(11,10)
L_1	2	0	0	1	3
L_2	4.24	0	4.47	0	0
L_3	0	2	1	2	2
L_4	0	3.61	0	0	0
L_5	2	0	0	1	3
L_6	4.24	0	4.47	0	0
L_7	0	0	1	2	2
L_8	0	5.39	0	0	0
A_1	2	0	0	1	3
A_2	4.24	0	4.47	0	0
A_3	0	1	1	2	2
A_4	0	4.50	0	0	0
Major axis orientation	−45°	61.43°	−63.43°	90°	0°
Major axis length	4.24	4.50	4.47	2	3
Area a	12	6	6	6	12
Row centroid $\bar{r}$	2.5	5.5	7.5	1.83	12
Column centroid $\bar{c}$	11.5	2.33	8.0	2.5	12.5
Gray level mean μ	8.0	4.0	6.33	3.83	3.42
Gray level variance σ^2	1.82	6.4	.82	7.77	6.45
Minor axis orientation	0°	90°	90°	0°	90°
Minor axis length	2	1	1	1	2

3.3 Signature Properties

We assume here that we are able to obtain, as discussed in Chapter 2, the required projections for any designated region R of an image. The projections are easily obtainable in pipeline hardware (Sanz, 1985; Sanz and Dinstein, 1987). The projections have been used in diverse applications, including character recognition (Breuer and Vajta, 1975; Spinrad, 1965; Pavlidis, 1968; Nakimoto et al., 1973; Yamamoto and Mori, 1978; Fujita, Nakanishi, and Miyata, 1976), shape analysis and recognition (Ma and Kusic, 1979; Wang, 1975; Pavlidis, 1978; Wong and Steppe, 1969), corner detection (Wu and Rosenfeld, 1983), chromosome recognition (Rutovitz, 1970; Klinger, Koehman, and Alexandridis, 1971), and cytology (Preston, 1976), to name a few. We will show how properties obtainable from vertical, horizontal, and diagonal projections include area, centroid of the region, second moments, and bounding rectangle. Then we will illustrate the use of signature analysis to determine the orientation and position of a rectangle and the position of a circle.

First we recall the definition of projections and show how to compute the properties just mentioned from the projections. The vertical projection P_V is defined by

$$P_V(c) = \#\{r|(r, c) \in R\}$$

The horizontal projection P_H is defined by

$$P_H(r) = \#\{c|(r, c) \in R\}$$

There are two diagonal projections: one going from lower left to upper right and one going from upper left to lower right. The diagonal projection P_D goes from lower left to upper right and is defined by

$$P_D(d) = \#\{(r, c) \in R|r + c = d\}$$

The diagonal projection P_E goes from upper left to lower right and is defined by

$$P_E(e) = \#\{(r, c) \in R|r - c = e\}$$

The area A can be obtained from any projection. For example,

$$A = \sum_{(r,c)\in R} 1 = \sum_{r} \sum_{\{c|(r,c)\in R\}} 1$$
$$= \sum_{r} P_H(r)$$

The top row, rmin, of the bounding rectangle is given by

$$\text{rmin} = \min\{r|(r, c) \in R\}$$
$$= \min\{r|P_H(r) \neq 0\}$$

The bottom row, rmax, of the bounding rectangle is given by

$$\text{rmax} = \max\{r|(r, c) \in R\}$$
$$= \max\{r|P_H(r) \neq 0\}$$

The leftmost column, cmin, of the bounding rectangle is given by

$$\begin{aligned}\text{cmin} &= \min\{c \,|\, (r,\ c) \in R\} \\ &= \min\{c \,|\, P_V(c) \neq 0\}\end{aligned}$$

The rightmost column, cmax, of the bounding rectangle is given by

$$\begin{aligned}\text{cmax} &= \max\{c \,|\, (r,\ c) \in R\} \\ &= \max\{c \,|\, P_V(c) \neq 0\}\end{aligned}$$

The row centroid $\bar{r}$ can be obtained from the horizontal projection P_H, as shown by the following straightforward calculation.

$$\begin{aligned}\bar{r} &= \frac{1}{A} \sum_{(r,\, c) \in R} r \\ &= \frac{1}{A} \sum_{r} \sum_{\{c \,|\, (r,\, c) \in R\}} r \\ &= \frac{1}{A} \sum_{r} r \sum_{\{c \,|\, (r,\, c) \in R\}} 1 \\ &= \frac{1}{A} \sum_{r} r P_H(r)\end{aligned}$$

The column centroid $\bar{c}$ can be obtained from the vertical projection P_V as follows:

$$\begin{aligned}\bar{c} &= \frac{1}{A} \sum_{(r,\, c) \in R} c \\ &= \frac{1}{A} \sum_{c} \sum_{\{r \,|\, (r,\, c) \in R\}} c \\ &= \frac{1}{A} \sum_{c} c \sum_{\{c \,|\, (r,\, c) \in R\}} 1 \\ &= \frac{1}{A} \sum_{c} c\, P_V(c)\end{aligned}$$

The diagonal centroid $\bar{d}$ can be obtained from the diagonal projection P_D.

$$\bar{d} = \frac{1}{A} \sum_{d} d\, P_D(d)$$

The diagonal centroid $\bar{e}$ can be obtained from the diagonal projection P_E.

$$\bar{e} = \frac{1}{A} \sum_{e} e\, P_E(e)$$

The diagonal centroid $\bar{d}$ is related to the row and column centroid

$$\begin{aligned}
\bar{d} &= \frac{1}{A}\sum_{d} d \sum_{\{(r,c)\in R | r+c=d\}} 1 \\
&= \frac{1}{A}\sum_{d} \sum_{\{(r,c)\in R | r+c=d\}} (r+c) \\
&= \frac{1}{A}\sum_{d} \sum_{\{(r,c)\in R | r+c=d\}} r + \frac{1}{A}\sum_{d} \sum_{\{(r,c)\in R | r+c=d\}} c \\
&= \frac{1}{A}\sum_{(r,c)\in R} r + \frac{1}{A}\sum_{(r,c)\in R} c \\
&= \bar{r} + \bar{c}
\end{aligned}$$

Similarly, the diagonal centroid $\bar{e}$ is related to the row and column centroid

$$\bar{e} = \bar{r} - \bar{c}$$

The second row moment μ_{rr} can be obtained from the horizontal projection P_H.

$$\begin{aligned}
\mu_{rr} &= \frac{1}{A}\sum_{(r,c)\in R} (r-\bar{r})^2 \\
&= \frac{1}{A}\sum_{r} \sum_{\{c|(r,c)\in R\}} (r-\bar{r})^2 \\
&= \frac{1}{A}\sum_{r} (r-\bar{r})^2 \sum_{\{c|(r,c)\in R\}} 1 \\
&= \frac{1}{A}\sum_{r} (r-\bar{r})^2 P_H(r)
\end{aligned}$$

Likewise, the second column moment μ_{cc} can be obtained from the vertical projection P_V.

$$\begin{aligned}
\mu_{cc} &= \frac{1}{A}\sum_{(r,c)\in R} (c-\bar{c})^2 \\
&= \frac{1}{A}\sum_{c} \sum_{\{r|(r,c)\in R\}} (c-\bar{c})^2 \\
&= \frac{1}{A}\sum_{c} (c-\bar{c})^2 \sum_{\{r|(r,c)\in R\}} 1 \\
&= \frac{1}{A}\sum_{c} (c-\bar{c})^2 P_V(c)
\end{aligned}$$

The second diagonal moment μ_{dd} can be obtained from the diagonal projection P_D.

$$\mu_{dd} = \frac{1}{A}\sum_{d} (d-\bar{d})^2 P_D(d)$$

The second diagonal moment μ_{dd} is related to μ_{rc}, μ_{rr}, and μ_{cc}.

$$\begin{aligned}\mu_{dd} &= \frac{1}{A}\sum_{d}\sum_{\{(r,c)\in R | r+c=d\}}(r+c-\bar{r}-\bar{c})^2 \\ &= \frac{1}{A}\sum_{(r,c)\in R}[(r-\bar{r})+(c-\bar{c})]^2 \\ &= \frac{1}{A}\sum_{(r,c)\in R}(r-\bar{r})^2+2(r-\bar{r})(c-\bar{c})+(c-\bar{c})^2 \\ &= \mu_{rr}+2\mu_{rc}+\mu_{cc}\end{aligned}$$

Hence the second mixed moment can be obtained from the second diagonal moment μ_{dd} by

$$\mu_{rc} = \frac{\mu_{dd}-\mu_{rr}-\mu_{cc}}{2}$$

The second diagonal moment μ_{ee} is also related to μ_{rc}, μ_{rr}, and μ_{cc}.

$$\begin{aligned}\mu_{ee} &= \frac{1}{A}\sum_{e}\sum_{\{(r,c)\in R | r-c=e\}}(r-c-\bar{r}+\bar{c})^2 \\ &= \frac{1}{A}\sum_{(r,c)\in R}[(r-\bar{r})-(c-\bar{c})]^2 \\ &= \frac{1}{A}\sum_{(r,c)\in R}(r-\bar{r})^2-2(r-\bar{r})(c-\bar{c})+(c-\bar{c})^2 \\ &= \mu_{rr}-2\mu_{rc}+\mu_{cc}\end{aligned}$$

Hence the second mixed moment can also be obtained from the second diagonal moment μ_{ee} by

$$\mu_{rc} = \frac{\mu_{rr}+\mu_{cc}-\mu_{ee}}{2}$$

The relationship between the two diagonal moments μ_{dd} and μ_{ee} implies that the mixed moment μ_{rc} can be obtained directly from μ_{dd} and μ_{ee}.

$$\mu_{rc} = \frac{\mu_{dd}-\mu_{ee}}{4}$$

3.3.1 Using Signature Analysis to Determine the Center and Orientation of a Rectangle

Signature analysis is important because of its easy, fast implementation. Many problems in industrial application can be solved with signature analysis. In SMD circuit board inspection, one inspection task is concerned with the position and orientation of rectangular parts and the position of circular parts. If 16 parts, for example, can be in one image frame, then in one frame time, video-rate hardware may com-

may compute the signatures for 16 parts. In this section we show how signature analysis can be used for rectangular parts. In the next section we show how it can be used for circular parts.

To determine the center and orientation of a rectangular region of known size by signature analysis, such as in Fig. 3.12, we can partition the rectangle into six regions formed by two vertical lines, a known distance g apart, and one horizontal line, as shown in Figure 3.13. This partition constitutes the projection index image. We assume that the corners of the rectangle are guaranteed to be in the extreme sextants of the partition. That is, the upper left-hand corner is in the sextant labeled A in Fig. 3.14, the lower left-hand corner, in the sextant labeled B; the upper right-hand corner, in the sextant labeled C; and the lower right-hand corner, in the sextant labeled D. Consistent with the model-based approach, the height h and width w of the rectangle are assumed known. The sextant partition constitutes the projection index image. The area of intersection of the rectangle with each sextant is determined by masking the projection index image with the binary image of the rectangle, as discussed in Section 2.4. A histogram of the masked projection image (the signature) then provides the area of intersection of each sextant with the rectangle. The problem is how to use the six area numbers to determine the units and orientation of the rectangle.

To solve the problem, set up a local x-,y-coordinate system whose origin is in the center of the six-celled partition. In actual practice there might be many

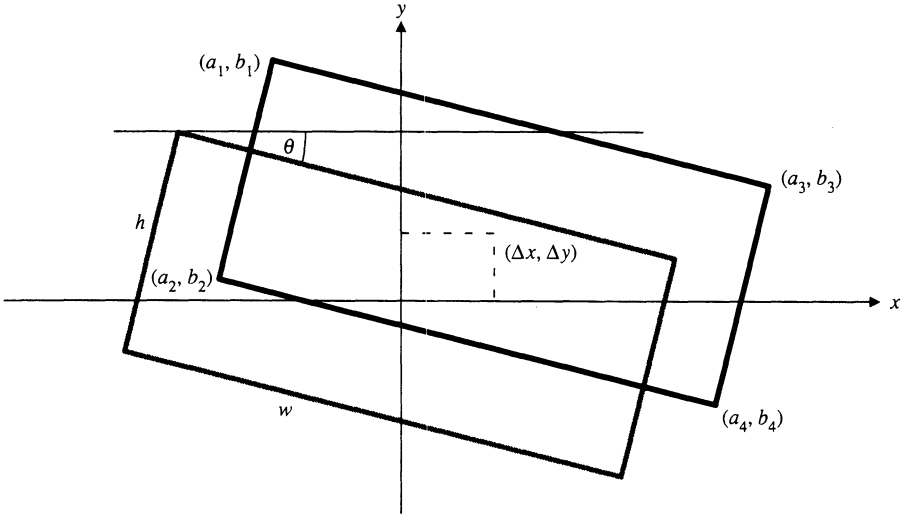

$$\begin{pmatrix} \Delta x \\ \Delta y \end{pmatrix} = \begin{pmatrix} a_1 + \frac{w}{2}\cos\theta - \frac{h}{2}\sin\theta \\ b_1 + \frac{w}{2}\sin\theta - \frac{h}{2}\cos\theta \end{pmatrix}$$

Figure 3.12 Geometry for determining the translation of the center of a rectangle in terms of the location of one corner, the length of its sides, and its orientation angle.

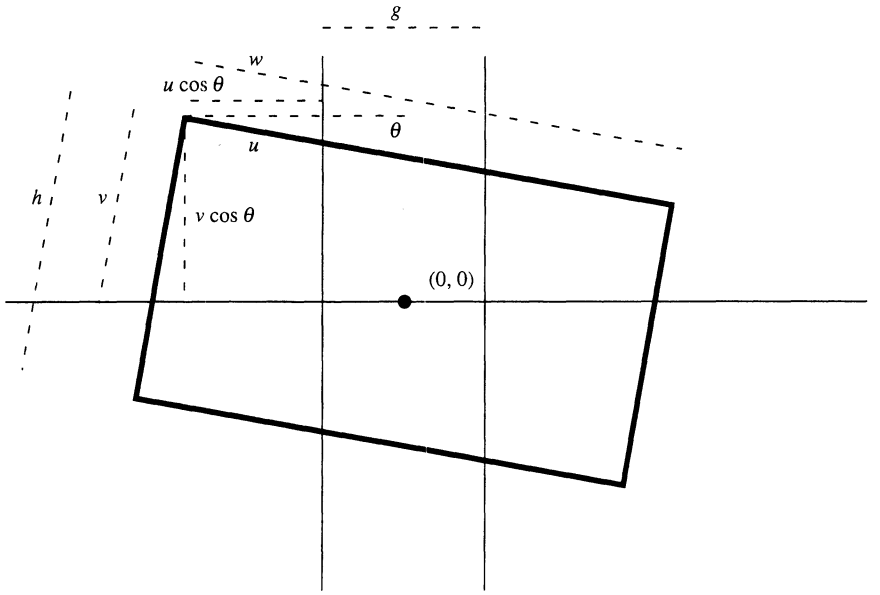

$$\begin{pmatrix}\Delta x\\ \Delta y\end{pmatrix} = \begin{pmatrix}\frac{-g}{2} - u\cos\theta + \frac{w}{2}\cos\theta - \frac{h}{2}\sin\theta\\ v\cos\theta - \frac{w}{2} - \sin\theta - \frac{h}{2}\cos\theta\end{pmatrix}$$

Figure 3.13 Geometry for determining the translation of the center of a rectangle in terms of the lengths u and v.

partitions on the image, one for the determination of each part in the image. We first suppose that the coordinates (a_1, b_1) of the upper left-most corner are known and that the orientation angle θ that the side of length w makes with the horizontal line is known. We solve for the coordinates $(\Delta x, \Delta y)$ of the center of the rectangle as follows.

First we determine the coordinate $(\Delta x, \Delta y)$ of the center of the rectangle in terms of the line segment length v from the upper left corner of the rectangle to the horizontal line and the line segment length u from the upper left corner of the rectangle to the left-most vertical line. From the geometry shown in Figure 3.13, we immediately have the results.

For a clockwise rotation of θ, a point (x, y) is rotated to the point (x_{rot}, y_{rot}), where

$$\begin{pmatrix}x_{rot}\\ y_{rot}\end{pmatrix} = \begin{pmatrix}\cos\theta & \sin\theta\\ -\sin\theta & \cos\theta\end{pmatrix}\begin{pmatrix}x\\ y\end{pmatrix}$$

For a rotation and shift of $(\Delta x, \Delta y)$, the point (x, y) becomes the point $(x_{\text{new}}, y_{\text{new}})$, where

$$\begin{pmatrix}x_{\text{new}}\\ y_{\text{new}}\end{pmatrix} = \begin{pmatrix}x_{rot}\\ y_{rot}\end{pmatrix} + \begin{pmatrix}\Delta x\\ \Delta y\end{pmatrix}$$

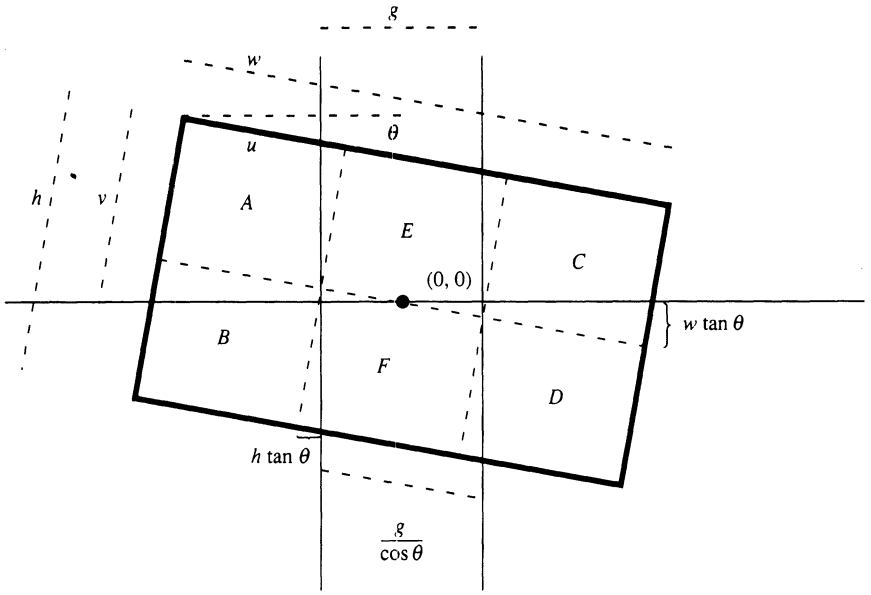

Figure 3.14 Geometry for determining the lengths u and v in terms of the measured areas A, B, C, D, E, and F.

For the case of the corner (a_1, b_1), we have from Figure 3.12

$$\begin{pmatrix} a_1 \\ b_1 \end{pmatrix} = \begin{pmatrix} \cos\theta & \sin\theta \\ -\sin\theta & \cos\theta \end{pmatrix} \begin{pmatrix} \frac{-w}{2} \\ \frac{h}{2} \end{pmatrix} + \begin{pmatrix} \Delta x \\ \Delta y \end{pmatrix}$$
$$= \begin{pmatrix} \frac{-w}{2}\cos\theta + \frac{h}{2}\sin\theta \\ \frac{w}{2}\sin\theta + \frac{h}{2}\cos\theta \end{pmatrix} + \begin{pmatrix} \Delta x \\ \Delta y \end{pmatrix}$$

from which it immediately follows that

$$\begin{pmatrix} \Delta x \\ \Delta y \end{pmatrix} = \begin{pmatrix} a_1 + \frac{w}{2}\cos\theta - \frac{h}{2}\sin\theta \\ b_1 - \frac{w}{2}\sin\theta - \frac{h}{2}\cos\theta \end{pmatrix}$$

Upon substituting $-g/2 - u\cos\theta$ for a_1 and $v\cos\theta$ for b_1, we obtain

$$\begin{pmatrix} \Delta x \\ \Delta y \end{pmatrix} = \begin{pmatrix} \frac{-g}{2} - u\cos\theta + \frac{w}{2}\cos\theta - \frac{h}{2}\sin\theta \\ v\cos\theta - \frac{w}{2}\sin\theta - \frac{h}{2}\cos\theta \end{pmatrix} \tag{3.6}$$

Next we determine the lengths u and v in terms of the measured areas A, B, C, D, E, and F as shown in Figure 3.14. From the geometry we can directly derive the appropriate equations.

From Fig. 3.14 we have

$$A + B = uh + \frac{1}{2}h^2\tan\theta$$
$$C + D = \left(w - \frac{g}{\cos\theta} - u\right)h - \frac{1}{2}h^2\tan\theta$$

We use both equations to maintain symmetry and numerical stability to determine an expression for u. Subtracting the first from the second,

$$(C+D)-(A+B)=\left(w-\frac{g}{\cos\theta}\right)h-2uh-h^2\tan\theta$$

Bringing the $2uh$ term as the sole term on one side of the equation, yields

$$2uh=-(C+D)+(A+B)+\left(w-\frac{g}{\cos\theta}\right)h-h^2\tan\theta$$

Hence

$$u=\frac{(A+B)-(C+D)}{2h}+\frac{1}{2}\left(w-\frac{g}{\cos\theta}\right)-\frac{1}{2}h\tan\theta \tag{3.7}$$

Also from Figure 3.14 we have

$$A+E+C=vw-\frac{1}{2}w^2\tan\theta$$
$$B+F+D=(h-v)w+\frac{1}{2}w^2\tan\theta$$

Again we use both equations to maintain symmetry and numerical stability to determine an expression for v. Subtracting one from the other, we obtain

$$\begin{aligned}(A+E+C)-(B+F+D)&=vw-\frac{1}{2}w^2\tan\theta-hw+vw-\frac{1}{2}\tan\theta\\&=2vw-hw-w^2\tan\theta\end{aligned}$$

Solving for v yields

$$\begin{aligned}2vw&=(A+E+C)-(B+F+D)+hw+w^2\tan\theta\\v&=\frac{(A+E+C)-(B+F+D)}{2w}+\frac{h}{2}+\frac{w}{2}\tan\theta\end{aligned} \tag{3.8}$$

Substituting the derived values of u and v from Eqs. (3.7) and (3.8) in terms of the measured area A,B,C,D,E, and F into Eq. (3.6) for the rectangle center, we have for Δx

$$\Delta x=\frac{g}{2}-u\cos\theta+\frac{w}{2}\cos\theta-\frac{h}{2}\sin\theta$$
$$\Delta x=\frac{g}{2}-\left[\frac{(A+B)-(C+D)}{2h}+\frac{1}{2}\left(w+\frac{g}{\cos\theta}\right)-\frac{1}{2}h\tan\theta\right]\cos\theta+\frac{w}{2}\cos\theta-\frac{h}{2}\sin\theta$$
$$\Delta x=\frac{(C+D)-(A+B)}{2h}\cos\theta$$

And for Δy

$$\begin{aligned}\Delta y &= v\cos\theta - \frac{w}{2}\sin\theta - \frac{h}{2}\cos\theta \\ &= \left[\frac{(A+E+C)-(B+F+D)}{2w} + \frac{h}{2} + \frac{w}{2}\tan\theta\right]\cos\theta - \frac{w}{2}\sin\theta - \frac{h}{2}\cos\theta \\ &= \frac{(A+E+C)-(B+F+D)}{2w}\cos\theta + \frac{h}{2}\cos\theta + \frac{w}{2}\sin\theta - \frac{w}{2}\sin\theta - \frac{h}{2}\cos\theta \\ &= \frac{(A+E+C)-(B+F+D)}{2w}\cos\theta\end{aligned}$$

Finally, it is easy to determine the rotation angle θ in terms of the areas E and F, which constitute a parallelogram. From the geometry it is obvious that

$$E+F = \frac{hg}{\cos\theta}$$

from which

$$\cos\theta = \frac{hg}{E+F}$$

3.3.2 Using Signature Analysis to Determine the Center of a Circle

To determine the center position of a circular region from signature analysis, we first partition the circle into four quadrants formed by two orthogonal lines guaranteed to meet inside the circle; then we measure the area in each quadrant from the histogram of the masked projection index image that consists of the four quadrants of a circle. To understand how to convert the area measurements into position information, consider the situation resulting when a chord partitions a circle into two regions A and B. Suppose the chord is a distance d from the circle center and that the radius of the circle is r.

Let θ be the angle between the perpendicular bisector of the chord and a line segment from the chord to the circle center (Fig. 3.15). Then the total area of the two right triangles is $d\sqrt{r^2-d^2}$ and the area of the sector with central angle 2θ and radius r is $r^2\theta$. The angle θ is given by $\theta = \cos^{-1}\frac{d}{r}$. Therefore the area of the segment determined by the chord and the circle circumference is

$$\begin{aligned}A &= r^2\cos^{-1}\frac{d}{r} - d\sqrt{r^2-d^2} \\ &= r^2\left[\cos^{-1}\frac{d}{r} - \frac{d}{r}\sqrt{1-\left(\frac{d}{r}\right)^2}\right]\end{aligned}$$

Noting that $\theta = \cos^{-1}\frac{d}{r}$, we can rewrite the segment area.

$$A = \frac{r^2}{2}[2\theta - \sin 2\theta]$$

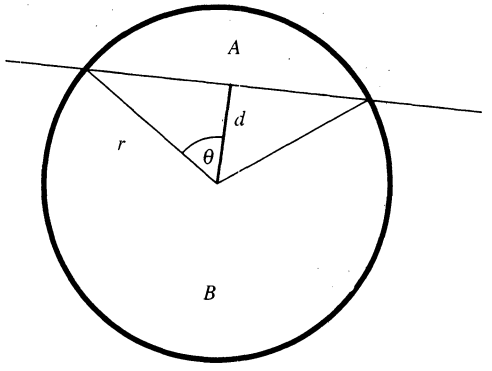

Figure 3.15 Geometry for the circle, its center, and a chord.

The total area of the circle is

$$A + B = \pi r^2$$

Hence the radius of the circle can be determined by

$$r = \sqrt{\frac{A+B}{\pi}}$$

Using this in the expression for the segment area, we obtain

$$\frac{2\pi A}{A+B} = 2\theta - \sin 2\theta$$

This transcendental equation has no closed-form solution for θ. It can be approximately solved for θ by a table-look-up technique. Then once θ has been computed, the offset d is determined by

$$d = \sqrt{\frac{A+B}{\pi}} \cos\theta$$

Now we are ready to consider the original problem of determining the center of a circle in unknown position. Measure the areas $A, B, C,$ and D (Fig. 3.16).

If $A + B > C + D$, then the y-coordinate of the circle's center is positive; otherwise it is negative. If $B + D > A + C$, then the x-coordinate of the circle's center is positive; otherwise it is negative.

The magnitude of the y-coordinate is given by

$$|\Delta y| = \sqrt{\frac{A+B+C+D}{\pi}} \cos\theta_y$$

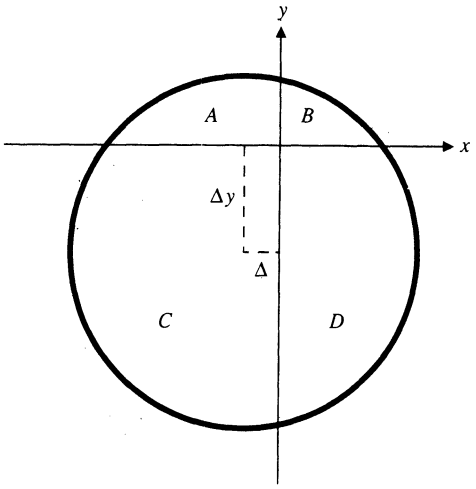

Figure 3.16 Circle projected onto the four quadrants of the projection index image.

where θ_y satisfies

$$\frac{2\pi(A+B)}{A+B+C+D} = 2\theta_y - \sin 2\theta_y$$

The magnitude of the x-coordinate is given by

$$|\Delta x| = \sqrt{\frac{A+B+C+D}{\pi}} \cos\theta_x$$

where θ_x satisfies

$$\frac{2\pi(B+D)}{A+B+C+D} = 2\theta_x - \sin 2\theta_x$$

3.4 Summary

In this chapter we have discussed a set of important properties of regions obtained from connected components or signature analysis. The properties have included spatial moments and mixed spatial gray level moments as well as extremal points. We have illustrated how it is possible to infer from the extremal points the sizes and orientation of linelike, trianglelike, rectanglelike, and octagonlike regions. Finally, we have shown how signature analysis can be used to determine the center and orientation of a rectangle and the center of a circle.

Exercises

3.1. Consider an elongated region whose extremal points are given by

(r_1, c_1)	(24, 137)	(r_5, c_5)	(39, 155)
(r_2, c_2)	(24, 163)	(r_6, c_6)	(39, 145)
(r_3, c_3)	(30, 181)	(r_7, c_7)	(32, 119)
(r_4, c_4)	(32, 181)	(r_8, c_8)	(30, 119)

Determine $M_1, M_2, M_3, M_4, \phi_1, \phi_2, \phi_3$ and ϕ_4. If this region is considered to be a rectangle, what would the computed orientation, length, and width of the rectangle be? What is the problem with assuming a rectangle model for a region whose shape does not satisfy the assumed model?

3.2. Determine the value of $||P||^2/A$ for a regular planar polygon having N sides and show that it is always greater than the value of $||P||^2/A$ for a circle.

3.3. Show that for a regular polygon of N sides the mean radii between the centroid and the boundary is given by

$$\mu_R = \frac{Nb}{\pi} \log \left(\frac{1 + \sin \pi/N}{\cos \pi/N} \right)$$

where b is the perpendicular distance between the polygon centroid and one of its sides.

3.4. Show that for a regular polygon of N sides the standard deviation of the radii between the centroid and the boundary is given by

$$\sigma_R = \frac{Nb}{\pi} \left[\frac{\pi}{N} \tan \frac{\pi}{N} - \log^2 \left(\frac{1 + \sin \pi/N}{\cos \pi/N} \right) \right]^{\frac{1}{2}}$$

3.5. Write a computer program to construct binary digital images of a digital circle or a digital diamond. Digital circles are specified by their radius and digital diamonds by the length of their sides. For any generated figure determine the value of $||P||^2/A$ where the length of the perimeter is the number of interior border pixels that are 4-adjacent to the background. Compare the values of $||P||^2/A$ for digital circles and digital diamonds by graphing each as a function of A.

3.6. A rectangle of width W and length L has an unknown orientation θ, where θ is the angle between the horizontal axis and the side of length L. A connected component analysis of an image of the rectangle measures the width W_B and length L_B of the bounding rectangle. Show that the orientation of the rotated rectangle satisfies

$$\sin 2\theta = \frac{2(W_B L_B - WL)}{W^2 + L^2}$$

3.7. Perform the following experiment to determine the accuracy of the signature analysis technique of Section 3.3.1 for determining the center and orientation of a rectangle as a function of noise and scale. Fix the rectangle to be L pixels in length by W pixels in width and the sextant partition to have a middle sextant of length $\frac{L}{3}$ pixels. Orient the rectangle so that the length L side is horizontal. Then choose a random rotation θ between -45° and 45° and a random translation (r, c) for row and column between $\frac{-L}{6}$ and $\frac{L}{6}$ pixels. Finally, with probability p, change a 0-pixel to a 1-pixel or a 1-pixel to a 0-pixel. With the noisy rectangle use the signature

analysis technique to estimate the position of the center $(\hat{r},\hat{c})$ of the rectangle and its orientation $\hat{\theta}$. Repeat the experiment 100 times observing $(\hat{r}_i,\hat{c}_i,\hat{\theta}_i), i = 1,\ldots,100$. Define

$$d_t = \sqrt{\frac{1}{100}\sum_{i=1}^{100}(r_i-\hat{r}_i)^2+(c_i-\hat{c}_i)^2} \quad \text{and} \quad d_\theta = \frac{1}{100}\sum_{i=1}^{100}|\hat{\theta}_i-\theta_i|,$$

where (r_i,c_i) is the true position of the ith rectangle. Plot d_t and d_θ as a function of noise parameter p. Change L and W and repeat the experiments. Compare the results.

3.8. Perform the following experiment to determine the accuracy of the signature analysis techniques of Section 3.3.2 for determining the center of a circular region. Generate circular regions having radius r. With probability p, change a 0-pixel to a 1-pixel or a 1-pixel to a 0-pixel. With the noisy circle, use the signature analysis technique to estimate the position of the center $(\hat{r},\hat{c})$ of the circle. Repeat this experiment 100 times observing $(\hat{r}_i,\hat{c}_i)$, $i = 1,\ldots,100$. Define

$$d_t = \sqrt{\frac{1}{100}\sum_{i=1}^{100}(r_i-\hat{r}_i)^2+(c_i-\hat{c}_i)^2}$$

Plot d_t as a function of noise parameter p and radius r.

3.9. Determine the extremal points of the ellipse $(x-x_c)'A(x-x_c) = 1$, where $x_c = \binom{5}{7}$ and

$$A = \frac{1}{146}\begin{pmatrix} 10 & -2 \\ -2 & 15 \end{pmatrix}$$

3.10. Consider an ellipse defined by $x'Ax = 1$, where

$$A = \begin{pmatrix} d & e \\ e & f \end{pmatrix}.$$

Show that the major axis length can be given by

$$\frac{\sqrt{2}\sqrt{d+f+\sqrt{(d-f)^2+4e^2}}}{\sqrt{df-e^2}}$$

and the minor axis length can be given by

$$\frac{\sqrt{2}\sqrt{d+f-\sqrt{(d-f)^2+4e^2}}}{\sqrt{df-e^2}}$$

3.11. Write a program that inputs a connected component image and outputs a property vector for each connected component. The property vector should have components of area, perimeter, centroid, orientation of fitted ellipse, length of major axis, length of minor axis, extremal points, standard deviation of the distance between centroid and boundary, and mean distance between centroid and boundary.

3.12. Write a program that generates binary images having nontouching squares and circles. Make the squares have random orientation. Make a histogram of the values for each property for the square regions and for the circle regions. What property looks most promising to distinguish circles from squares? How large do the squares and circles

have to be before it becomes easy to distinguish a square from a circle by using the standard deviation of the distance between the centroid and boundary and the mean distance between centroid and boundary?

Bibliography

Breuer, P., and M. Vajta, "Structural Chracter Recognition by Forming Projections," *Problems in Control Information Theory,* Vol. 4, 1975, pp. 339–352.

Fujita, T., M. Nakanishi, and K. Miyata, "The Recognition of Chinese Characters (Kanji) Using Time Variation of Peripheral Belt Patterns," *Proceedings of the Third International Joint Conference on Pattern Recognition,* Coronado, CA, 1976, pp. 119–121.

Gleason, G. J., and G. J. Agin, "A Modular Vision System for Sensor Controlled Manipulation and Inspection," *Proceedings of the Ninth International Symposium on Industrial Robots,* Washington, DC, March, 1979, pp. 57–70.

Haralick, R. M., "A Measure of Circularity of Digital Figures," *IEEE Transactions on Systems, Man, and Cybernetics,* Vol. SMC–4, 1974, pp. 394–396.

Haralick, R. M., K. Shanmugam, and I. Dinstein, "Textural Features for Image Classification," *IEEE Transactions on Systems, Man, and Cybernetics,* Vol. SMC–3, 1973, pp. 610–621.

Klinger, A., "Pattern Width at a Given Angle," *Communications of the ACM,* Vol. 14, 1971, pp. 21–25.

Klinger, A., A. Koehman, and N. Alexandridis, "Computing Analysis of Chromosome Patterns: Feature-Encoding for Flexible Decision Making," *IEEE Transactions on Computers,* Vol. C–20, 1971, pp. 1014–22.

Ma, K., and G. Kusic, "An Algorithm for Distortion Analysis in Two–Dimensional Patterns Using Its Projections," *Proceedings of the Seventh New England Bioengineering Conference,* Troy, NY, 1979, pp.177–180.

Nakimoto, Y., et al., "Improvement of Chinese Character Recognition Using Projection Profiles," *Proceedings of the First International Joint Conference on Pattern Recognition,* Washington, D.C., 1973, pp. 172–178.

Pavlidis, T., "Computer Recognition of Figures through Decomposition," *Information and Control,* Vol. 14, 1968, pp. 526–537.

——, *Structural Pattern Recognition,* Springer-Verlag, New York, 1977.

——, "Algorithms for Shape Analysis of Contours and Wave-Forms," *Proceedings of the Fourth International Conference on Pattern Recogntion,* Kyoto, Japan, 1978, pp. 70–85.

Preston, K., "Digital Picture Analysis in Cytology," *Digital Picture Analysis,* A. Rosenfeld (ed.), Springer-Verlag, New York, 1976, pp. 209–294.

Rosenfeld, A., "Compact Figures in Digital Pictures," *IEEE Transactions on Systems, Man, and Cybernetics,* Vol. SMC–4, 1974, pp. 221–223.

Rutovitz, D., "Centromere Finding: Some Shape Descriptors for Small Chromosome Outlines," *Machine Intelligence,* Vol. 5, 1970, pp. 435–462.

Sanz, J. L. C., "A New Method for Computing Polygonal Masks in Image Processing Pipeline Architectures," *Pattern Recognition,* Vol. 18, 1985, pp. 241–247.

Sanz, J. L. C., and I. Dinstein, "Projection–Based Geometrical Feature Extraction for Computer Vision: Algorithms in Pipeline Architectures," *IEEE Transactions on Pattern Analysis and Machine Intelligence,* Vol. PAMI–9, 1987, pp. 160–168.

Spinrad, R. J., "Machine Recognition of Hand Printing," *Information and Control,* Vol. 8, 1965, pp. 124–142.

Wang, Y. R., "Characterization of Binary Patterns and Their Projections," *IEEE Transactions on Computers,* Vol. C-24, 1985, pp. 1032–35.

Wong, E., and J. A. Steppe, "Invariant Recognition of Geometric Shapes," *Methodologies of Pattern Recognition,* S. Watanabe (ed.), Academic Press, New York, 1969, pp. 535–546.

Wu, Z. Q., and A. Rosenfeld, "Filtered Projections as an Aid in Corner Detection," *Pattern Recognition,* Vol. 16, 1983, pp. 31–38.

Yamamoto, K., and S. Mori, "Recognition of Handprinted Characters by Outermost Point Methods," *Proceedings of the Fourth International Conference on Pattern Recognition,* Kyoto, Japan, 1978, pp. 794–796.